Consensus-Based Voltage Restoration and Synchronization of Islanded Microgrid in the Presence of Communication Latency and Noise

S. A. Olayanju [1*], F. M. Dahunsi [2], A. A. Ponnle [3]

[1]Electrical and Electronics Engineering Department, University of Ilorin, Nigeria.
[2]Computer Engineering Department, The Federal University of Technology, Akure, Nigeria.
[3]Electrical and Electronics Engineering Department, The Federal University of Technology, Akure, Nigeria.

ABSTRACT: Secondary control of microgrids (MGs) commonly employs consensus algorithms over communication networks to coordinate control objectives across distributed units. However, communication delays and noise, can adversely affect the dynamic performance of the system and, in severe cases, compromise overall stability. This paper proposes a robust distributed secondary control strategy for inverter-based MGs operating within sparsely connected distribution networks. A consensus-based control framework is employed to achieve voltage synchronization among distributed generators (DGs) in an islanded MG. The control scheme leverages a detailed MG model to design a consensus-based secondary controller that compensates for voltage and local reactive power deviations, utilizing information exchanged over communication links subject to latency and noise disturbances. The effectiveness of the proposed control approach is validated through simulation studies conducted on a four-DG MG test system developed in the MATLAB/SimPowerSystems environment. Voltage restoration performance evaluated under the following delay conditions: $\tau_{t1} = 0.6$ s, $\tau_{t2} = 0.7$ s, $\tau_{t3} = 0.8$ s, and $\tau_{t4} = 1.0$ s, indicate that the time required by the system to reach synchronization increases proportionally with the level of delay. At a maximum latency of 1.0 s, the system achieves voltage consensus approximately 3.3 seconds. Under communication noise impairment with varying noise variances, specifically $\sigma^2 = 0.1, 0.2, 0.3$, and 0.4. Voltage synchronization was achieved across all scenarios, with an average convergence time of approximately 3 seconds. Results demonstrate that the proposed method effectively maintains voltage synchronization across the DGs under varying load conditions, even in the presence of communication impairments.

KEYWORDS: KEYWORDS: Voltage control, Latency, Noise, Microgrid, Consensus method, Multi-agent.

[Received Apr. 18 2025; Revised Apr. 28, 2025; Accepted Apr. 30, 2025] Print ISSN: 0189-9546 | Online ISSN: 2437-2110

I. INTRODUCTION

DC/AC electronic inverters used as interface between the microgrid (MG) and distributed energy resources (DER) allow the integration of many such DER in a MG system. Essentially, MGs operate in islanded mode when there is fault or disturbances in the system or when the utility grid is unavailable (Seyedmohammad Hasheminasab; et al., 2024; Yasir et al., 2024). Islanded MGs could also be designed on purpose to serve critical loads such as military installations, health care facility or education environment (Mallery et al., 2022). A grid-connected MG could take additional supply from the main grid or could be supporting power delivery of the grid. Autonomous MGs incorporates local primary control (droop technique) to maintain the operating frequency and voltage of the connected distributed generators (DG) during load perturbation in the autonomous mode of operation. To maintain the balance of output power in the MGs, each DG adjust its output accordingly (Dehkordi et al., 2019; Olayanju et al., 2024). However, some drawback associated with using primary droop control in MGs include inability to maintain fixed frequency, high dependence on line impedance, voltage and frequency deviations, poor power sharing among distributed generators (DGs) and system instability (Aghaee et al., 2019; Shrivastava et al., 2019; Wu et al., 2019). Secondary control is crucial in islanded MGs to mitigate the limitations associated with primary control methods and maintain stable operation (Andreotti et al., 2021; Lou et al., 2018; Pompodakis et al., 2024). Centralized secondary control, while effective in other applications, has significant drawbacks when used in MGs system. In centralized secondary control technique, information from individual DG is aggregated and processed at a central point before the control signal is disseminated to each DG (Olayanju et al., 2021). As a result, it suffers from single point of failure which could result in complete collapse of the MG system. Other drawbacks include: complex communication network, poor scalability and flexibility, high computational burden and sensitivity to communication delays (Aghaee et al., 2019; Chen, Xiao, 2018; Wu et al., 2019). Researchers have mostly replaced centralized control with distributed control in secondary control of MGs because of its improved reliability, reduced communication, enhanced flexibility, and resilience among others (Huang et al., 2024; Sheykhi et al., 2022).

*Corresponding author: fmdahunsi@futa.edu.ng *doi:* http://dx.doi.org/10.63746/njtd.v22i3.3610

The distributed approach to microgrid control involves each DG unit having its secondary controller to regulate voltage individually while communicating with neighboring units (Aghaee et al., 2019; Aluko et al., 2022). This approach combines the advantages of centralized and decentralized secondary controls (Aluko et al., 2022). Distributed control is inspired by cooperative control in multi-agent systems (Dehkordi et al., 2019; Shrivastava et al., 2019). Several methods have been implemented to achieve distributed control. To implement Distributed Secondary Control in MGs, Consensus-Based Methods which aim to bring different RES in the MG to a single value, achieve a global optimal value through communication links between adjacent RES without proprietary units was reported by (Aghaee et al., 2019; Sheykhi et al., 2022). The consensus algorithm, a distributed approach that has become popular for distributed control has been developed using local information exchange between neighbors through shared communication networks. In Multi-Agent Systems (MAS) approach, each DG is regarded as an intelligent agent, and the entire MG is a multi-agent system. Each DG exchanges information only with its adjacent DGs to achieve the control goal (Li et al., 2022). Distributed Model Predictive Control techniques provides explicit consideration of constraints, it is easy to tune and can handle multivariable control problems. It can realize secondary voltage control by incorporating the predicted behaviors of the local and neighboring DG units (Lou et al., 2018). However, implementation of the technique may involve some form of complexity. A feedback linearization approach can reduce the non-linear system into a linear system and convert the distributed voltage control into a tracking synchronization problem (Shrivastava et al., 2019). An intelligent method using fuzzy logic and Particle Swam Optimization (PSO) techniques can be used to control the MG frequency only using centralized control (Jasim et al., 2023). To ensure accurate reactive power sharing and reduce amplitude deviations, a networked control system has been studied (Ahmed et al., 2021).

In the aforementioned literature, all DERs are assumed to have unhindered access to system parameters and that communication impairments such as noise and delay between DERs are negligible. However, due impairments along the communication path, it becomes challenging for individual agent to obtain precise information from its neighbors. In this paper, a Consensus-Based Voltage Restoration and Synchronization of Islanded Microgrid is considered. The technique is robust in the presence of noise and communication delay while information is being exchanged among the communicating DGs. The remaining part of the paper is organized as follows: The problem is formulated in section II, graph theory basics is discussed in section III, multi-agent communication is described in section IV, and the communication link impairments are modeled in section V, the proposed secondary consensus-based secondary controller is in section. VI. Simulation study is presented in VII while the results obtained were presented and discussed in section VIII. The conclusion was drawn in section IX.

II. MATERIALS AND METHODS

The inverter-based microgrid is considered in this paper. A solar Photovoltaic (PV) is the energy source for the microgrid system. For the i_{th} Renewable Energy Source (RES), the primary controller, comprises of the conventional power droop, voltage and current controllers in a loop, as well as the secondary control procedure. The d-q reference frame transform of the original abc waveform is used in the primary control loop. The control procedure implemented during operation is as follows: the power droop control loop is fed with the nominal set points frequency (ω_{ni}) and voltage magnitude (e_{ni}). The power droop controller generates the reference values, ω_i^* and v_{odi}^*, which serves as the inputs of the voltage controller, the voltage loop generates the current reference, i_{ldi}^* and i_{lqi}^*, for the current control loop. Then, in the current controller, the current errors are determined and the voltage reference signals v_{ldi}^* and v_{lqi}^* generated are used to regulate the outputs of the inverter via Space Vector Pulse Wave Modulator (SVPWM) mode.

To mitigate the deviations in voltage and frequency as a result of the primary control procedure, the secondary control mechanism is implemented in a distributed manner to generate new nominal set points for RES. The multi-agent control scheme is used to design the secondary controller using the information shared among the neighboring RES to update ω_i^* and v_{odi}^* in each primary control process, and thus, restore the terminal output ω_{ni} and e_{ni} , to the desired reference values.

The multi-agent-based controller developed, utilizing the linear consensus protocol, was subjected to a comparative analysis with the conventional consensus protocol methods. Through this comparison, the performance of the smart microgrid (SMG) was evaluated and optimized. The primary controller comprises the power droop, voltage and current control units, connected in cascade as used by (Ali et al., 2017; Hu and Bhowmick, 2020; Pogaku et al., 2007). Its control structure is shown in Figure 1

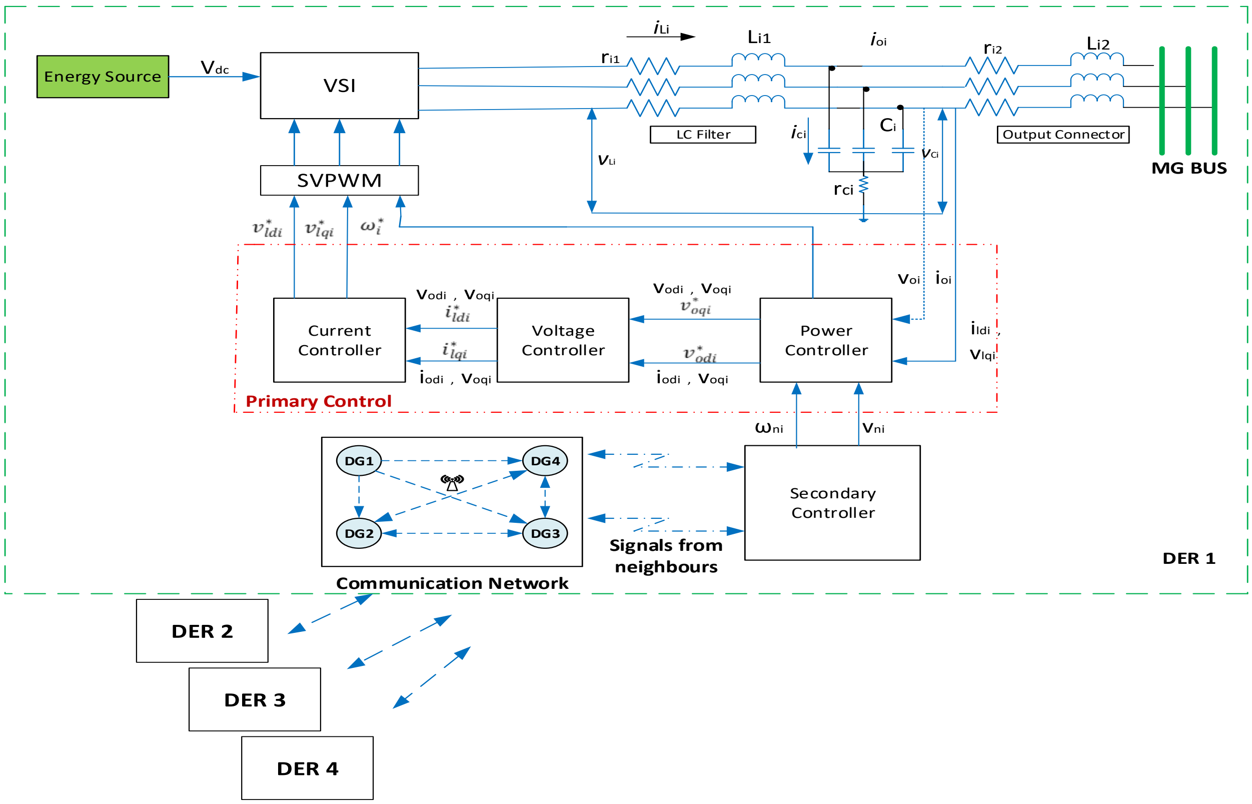

Figure 1: Microgrid control structure

III. GRAPH THEORY BASICS

In the context of multi-agent topology representation, directed (digraphs) or undirected graphs may be employed to facilitate distributed control among DG sources (agents). This describe the systematic manner in which the topology of an agent network is structured.

Provided that $\mathcal{G} = (\mathcal{V}, \mathcal{E}, \mathcal{A})$ is a weighted directed graph of order n, encompassing the collection of edges $\mathcal{E} \subseteq \mathcal{V} \times \mathcal{V}$, with set of nodes $\mathcal{V} = \{v_{1,} \dots . v_n\}$, and a weighted adjacency matrix $\mathcal{A} = [a_{ij}]$, in which the adjacency elements a_{ij} are non-negative. Every agent in a network is represented by one or more digraph nodes. The communication links between linked nodes are indicated by the edges. Agent i is implied to acquire information from agent j by each edge $\mathcal{E}_{ij} = (v_i, v_j)$ (Olfati-Saber and Murray, 2004; Zhang et al., 2017). An agent using a digraph only gets information from its neighbors N_i. The weight of edge $\mathcal{E}_{ij} = (v_i, v_j)$ is represented by a_{ij}, which equals 1 if $(v_i, v_j) \epsilon \mathcal{E}$ and 0 otherwise. The set of node $\mathcal{V}_i$ neighbors is indicated by:

$$N_i = \{v_j \epsilon v : (v_i, v_j) \epsilon \mathcal{E}\} \quad (1)$$

$\mathcal{D} = diag\{d_i\} \in R^{N \times N}$ is the definition of the in-degree matrix, where $d_i = \sum_{j \in N_i} a_{ij}$. An edge sequence representing a straight path from node i to node j is written as $\{(v_i, v_k),\ (v_k, v_l),\ \cdots, (v_m, v_j)\}$. Supposing agents in the network are connected using a communication graph. The control method requires a communication graph with adjacency, degree, and Laplacian matrices (Lou et al., 2020; Nasirian et al., 2015). The adjacency matrix, $\mathcal{A}(\mathcal{G})$, is formulated as:

$$\mathcal{A}(\mathcal{G}) = [a_{ij}] \begin{cases} 1 & v_i v_j \in N \\ 0 & otherwise \end{cases} \quad (2)$$

where a_{ij} is the communication weight (a design parameter), and N, the neighboring nodes. The minimum spanning tree (MST) ensures the optimal path for information exchange among the agents. The communication graph with MST must be constructed before communication can start. The MST must also be updated when a new agent joins the system (Lakshminarayanan et al., 2016). The communication graph should at least have a MST, be directional and carry the minimum redundancy. A degree of a vertex is denoted $d(v_i)$, in undirected graph $\mathcal{G}_r$, this is given by the number of adjacent vertices to v_i in the graph. The degree matrix, $\mathcal{D}(\mathcal{G})$, is a diagonal matrix where the diagonal elements is represented by the degree of each vertex (Ali et al., 2017). The degree matrix can be represented as shown in Equation 3:

$$\mathcal{D}(\mathcal{G}) = \begin{bmatrix} d(v_1) & 0 & \cdots & 0 \\ 0 & d(v_2) & \cdots & 0 \\ \vdots & \vdots & \ddots & \vdots \\ 0 & 0 & \cdots & d(v_n) \end{bmatrix} \quad (3)$$

The graph Laplacian matrix, $\mathcal{L}(\mathcal{G})$, associated with the degree and adjacency matrices, is given as

$$\mathcal{L}(\mathcal{G}) = \mathcal{D}(\mathcal{G}) - \mathcal{A}(\mathcal{G}) \quad (4)$$

The uniqueness of the Laplacian matrix, $\mathcal{L}(\mathcal{G})$ is described in the following:

$\mathcal{L}$ is positive semi-definite i.e., it takes up a real matrix $\mathcal{A}$ denoted as positive definite if and only if the eigenvalues of $\mathcal{A} + \mathcal{A}^T$ are non-negative. The smallest eigenvalue of $\mathcal{L}$ is zero, other eigenvalues are non-negative and real $(0 = \lambda_1 \leq \lambda_2 \leq \cdots \leq \lambda_n)$. And finally, the addition of individual Laplacian matrix row equals to zero.

IV. MULTI-AGENT COMMUNICATION

Figure 2 presents the communication architecture of the microgrid system, the four distributed generators (DGs) are interconnected via both electrical and communication links. During inter-DG data exchange, communication impairments, that is latency and noise are introduced alongside the transmitted information.

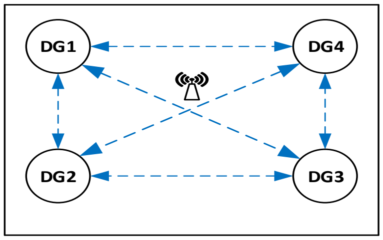

Figure 2: Graph topology for the communication network with full connectivity

The interactive matrix, a_{ij1}, representing the adjacency matrix of the communication topology among the distributed generators (DGs) in the microgrid, is defined in Equation (5). In the context of the consensus algorithm, the communication graph depicted in Figure 2 is assumed to be fully connected and undirected, enabling bidirectional information flow among all DGs. An edge weight of 1 denotes a strong communication link, which facilitates reliable and uniform information exchange necessary for achieving consensus across the network.

$$\mathcal{A}(\mathcal{G}) = \begin{bmatrix} 0 & 1 & 1 & 1 \\ 1 & 0 & 1 & 1 \\ 1 & 1 & 0 & 1 \\ 1 & 1 & 1 & 0 \end{bmatrix} \tag{5}$$

Equations 6 and 7 were used to develop degree and Laplacian matrices are derived.

$$\mathcal{D}(\mathcal{G}) = \begin{bmatrix} d(v_1) & 0 & \cdots & 0 \\ 0 & d(v_2) & \cdots & 0 \\ \vdots & \vdots & \ddots & \vdots \\ 0 & 0 & \cdots & d(v_n) \end{bmatrix} \tag{6}$$

where $d(v_i)$ is degree of a vertex and $\mathcal{L}(\mathcal{G})$, the graph Laplacian matrix, is defined as

$$\mathcal{L}(\mathcal{G}) = \mathcal{D}(\mathcal{G}) - \mathcal{A}(\mathcal{G}) \tag{7}$$

A. Algorithm for DGs Communication

Assumptions: All multi-agent units operate within mutual communication range, ensuring continuous inter-agent communication. Furthermore, all units are time-synchronized based on the communication timestamps. Precision synchronization at the packet level is required to maintain temporal consistency across the network.

Let τ be the time instant.

At ith time instant, distributed generator DG_j is in a transmitting state while DG_i is receiving, under the condition that $j\epsilon N_i$ where N_i denotes the set of neighbors of node. The neighborhood set is formally defined in Equation (1), where ε, represents the set of communication edges interconnecting the agent nodes. Here, v_i and v_j correspond to the nodes associated with DG_i and DG_j respectively. This communication topology is assumed to be modeled by a connected communication graph that satisfies the properties of a minimum spanning tree (MST), ensuring reachability and minimal redundancy in communication links. At each discrete time instant, each distributed generator (DG) independently measures and transmits a set of local state variables. These parameters include the local voltage value, v_i and the reactive power output Q_i which are critical for synchronization and control within the distributed system.

The algorithm for consensus of multi-agent system is described as follows:

At the ith time instant, for DG_i, the locally measured parameters; voltage and reactive power, Q_i, are collectively represented by the state vector $x_i(\tau)$, where τ denotes the current time index. The local estimate of the global average of these measured parameters, as computed by DG_i at time τ, is denoted by $h_i(\tau)$. The communication signal transmitted by neighboring node DG_j at ith time instant is defined as follows:

$$T(\tau) = h_j(\tau);\ \ j\epsilon N_i \tag{8}$$

DG_j broadcasts its current state vector to all neighboring units Upon reception of the transmitted state, each neighboring DG_i utilizes the received information to update its local estimate of the global parameter according to the following update rule:

$$h_i(\tau) = x_i(\tau) + \delta x_i(\tau), \qquad i = 0, 1, \ldots. N-1 \tag{9}$$

δx_i is the local control signal estimated based on the last received transmitted signal $h_j(\tau)$.

$$h_j(\tau) = h_j(k) \tag{10}$$

k denotes the time instant at which the last successful transmitted signal has been received by agent DG_i.

V. COMMUNICATION LINK IMPAIRMENTS

A. Link Noise

Considering two agents (nodes), agent v_i, the receiver and agent v_j, the transmitter, communicating wirelessly. The following steps are taken to arrive at the model for communication link noise used in the simulation: Signal transmission: Node v_j transmit a signal $x_j(t)$, with power S; wireless channel: The signal travels through the wireless channel, which introduces noise, $n(t)$. Received Signal: Node v_i receives a signal $r(t)$, which is the sum of the original signal and noise: $r(t) = x_j(t) + n(t)$. Using the linear consensus protocol the expression for wireless communication link noise can be given as:

$$r_i(t) = \sum_{j \in N_i} a_{ij}\left[x_i(t) - x_j(t)\right] + n(t) \tag{11}$$

where $n(t)$ is the noise which represents Additive White Gaussian Noise (AWGN).

B. Link Time Delay

Using a graph network $\mathcal{G} = (v, \varepsilon, A)$ having a fixed topology. The trending information of node v_j is transmitted to v_i, a neighbouring node, via a communication link e_{ji}. Applying the linear consensus protocol, the delay dependent signal transmitted from node v_j is given as:

$$u_i(t) = \sum_{u_j \in N_i} a_{ij}\left[x_j(t - \tau_{ji}) - x_i(t - \tau_{ji})\right] \tag{12}$$

with consensus gain, $-K_{c,i}$, the state of the node at v_i can then be expressed as:

$$\dot{x}_i(t) = -K_{c,i} \sum_{u_j \in N_i} a_{ij}\left[x_j\left(t-\tau_{ji}\right) - x_i\left(t-\tau_{ji}\right)\right] \quad (13)$$

Assuming that $\psi_i \in \mathcal{R}$ denotes state variables (voltage magnitude, or reactive power) of ith agent, the information sharing process with time delay τ_{ij} can be expressed as:

$$\psi_i\left(t+\tau_{ij}\right) = \psi_i(t) + \sum_{j \in N_i} a_{ij}\psi_j(t) \quad (14)$$

for $i = 1, 2, \ldots .n$; $j = 1, 2, \ldots .n$; $\psi_i(t)$ and $\psi_i\left(t+\tau_{ij}\right)$ are the shared information by ith DG at iteration t and $t+\tau_{ij}$ respectively. $\psi_j(t)$ is the information shared by jth DG. a_{ij} is the adjacency matrix which represent the coefficient for information exchange between agent v_i and v_j. The global information sharing process of the microgrid can be expressed as:

$$\begin{cases} \psi\left(t+\tau_{ij}\right) = \mathcal{A}_{ij} \times \mu(t) \\ \tau_{ij} = \dfrac{n_{bit} \times n_p}{\mathcal{V}_{com}} + \left(\dfrac{d}{s}\right) \end{cases} \quad (15)$$

Here, $\mu(t)$ denotes the information-sharing matrix governing inter-agent data exchange. The term $\mathcal{A}_{ij}$ represents the update matrix, which is defined based on the underlying communication topology and characterizes the influence of agent j on agent i. The variable τ_{ij} denotes the communication delay associated with the transmission of information from DG_j to DG_i within a single iteration; this delay encompasses both network-induced latency and propagation delay. The n_p denotes the dimensionality in the information-sharing matrix. $\mathcal{V}_{com}$ is the data communication rate, expressed in bits per second (bps), while d represents the physical distance between communicating agents (DGs), and s is the signal propagation speed within the transmission medium. Fundamentally, Equation (15) accounts for two primary delay sources: (i) delays introduced by the communication network infrastructure (e.g., queuing, processing), and (ii) physical propagation delays imposed by the communication channel. For a robust and balanced communication link between agents v_i and v_j in the network graph, the matrix element $\mathcal{A}_{ij}$must satisfy the following condition:

$$\begin{cases} \sum_i a_{ij} = 1 \\ \sum_j a_{ij} = 1 \end{cases} \quad (16)$$

VI. PROPOSED CONSENSUS-BASED SECONDARY VOLTAGE CONTROL

The following assumptions were considered in the development of the consensus-based control system: i. each of the Distributed Generating (DG) unit is regarded as an "agent" which is capable of sharing information with other DGs in its neighbourhood. ii. each agent can also take control decisions based on the information received from the neighbours. iii. all participating agents aim to reach a consensus with the values being shared, and the reference value is the predetermined consensus value.

A. Voltage Synchronization

Given the frequency droop expressed by Equation 17

$$V_i = v_{ni} - n_{qi}Q_i \quad (17)$$

where V_i, is the rated system voltage, n_{qi} is the droop coefficient, and Q_i is the measured reactive power. v_{ni}, is the actual voltage from DGi. Using the shared variable, v_{ni}, and Q_i, the objective is to design δe_i, and δQ_i, the distributed voltage and reactive power controller respectively, that will satisfy:

$$\lim_{t \to \infty} \mathcal{V}_i(t) = \mathcal{V}_{MG} \quad i = 1, 2, \cdots, N \quad (18)$$

That is, to restore the frequency of each DG to the reference value, and as a result reach a consensus value for the microgrid optimal operation.

The second objective is to ensure optimal reactive power sharing among the DGs, that is;

$$nQ_1 = n_2Q_2 = \cdots = n_NQ_N, as\ t \to \infty \quad (19)$$

These objectives are to be achieved despite the effects of communication impairments considered in this paper. Using the consensus protocol and incorporating the outputs of neighbouring DGs, the voltage controller δe_i is written as:

$$\delta e_i = \int \left[C_1 \sum_{j \epsilon N_i} a_{ij}\left(v_j\left(t-\tau_{ij}\right) - v_i(t)\right) - g_i\left(v_i(t) - v_{ref}\right)\right] dt \quad (20)$$

where C_1 is a positive constant representing the coupling strength of the communication network, a_{ij} is the weighted adjacency matrix of the voltage, g_i is the pinning gain, which is 1 when the node is connected to the reference value or 0 otherwise.

B. Reactive Power Sharing

Using the consensus based algorithm, the objective of equal active power sharing could be achieved. The power sharing algorithm could be designed by incorporating relative active power among neighbouring DGs as follows:

$$\delta Q_i = \sum_{j \epsilon N_i} C_2 a_{ij}\left[n_j Q_j\left(t-\tau_{ij}\right) - n_i Q_i\right] / n_i \quad (21)$$

For all $i = 1,2, . \ . \ . \ . \ N$, where C_2 is a positive constant representing the coupling strength of the communication network, n_j and n_i are the constant droop coefficients of nodes v_j and v_i respectively. The eventual control signal is given by:

$$u_i^e = \delta e_i + \delta Q_i \quad (22)$$

The general framework for the multi-agent control system is given in Figure 3. The multi-agent control inputs have two parts, the part shown in (19), is the summation of the tracking errors in frequency based on the information from the neighbours. This component is employed for the correction of frequency deviation. The second part shown in (20) is the summation of the local active power tracking error with neighbours. This aspect is used to achieve improved active power sharing.

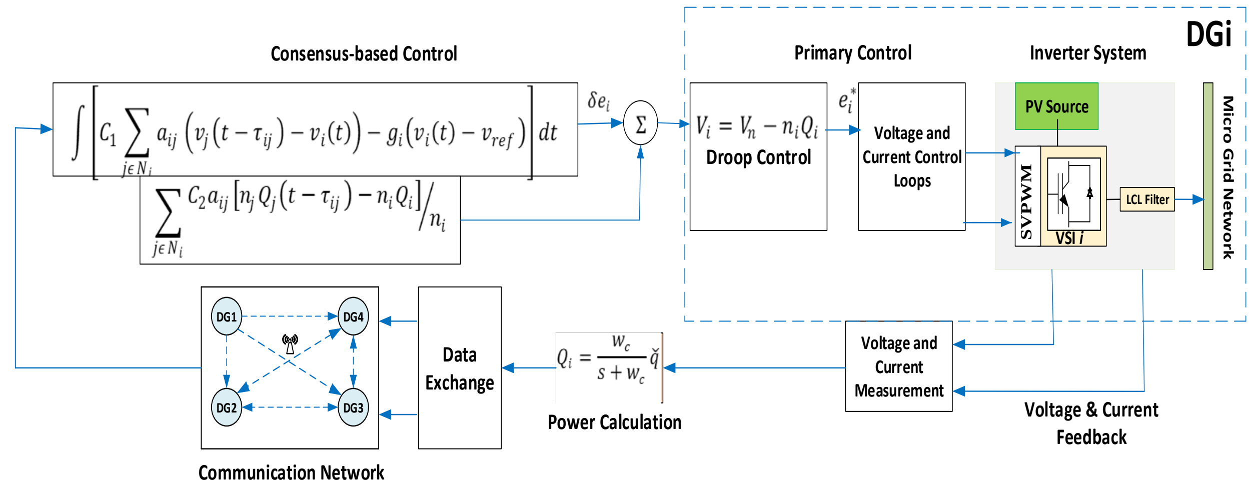

Figure 3: Framework for the consensus-based secondary voltage control scheme.

VII. SIMULATION STUDY

A four-inverter microgrid test system shown in Figure. 4, is prototyped in the MATLAB/SIMULINK software environment. The rated voltage and frequency are 240 V and 60 Hz respectively. Filters are connected at the inverters' outputs to reduce switching harmonics. Parameters used for simulations are given in Table 1.

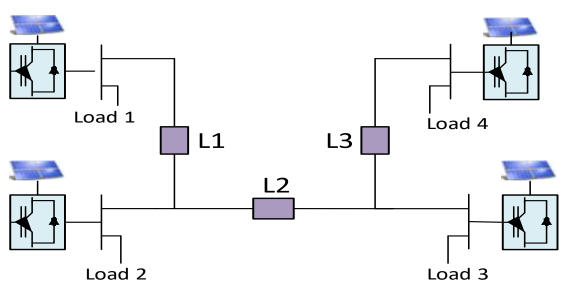

Figure 4: Single line diagram of the four-inverter microgrid

Table 1. Parameters for the microgrid test system.

DG1 and DG2		DG3 and DG4		Lines	R(Ω)	L(mH)
m_p	9.4e-5	m_p	12.5e-5	1	0.23	0.318
n_q	1.3e-3	n_q	1.5e-3	2	0.35	0.184
R_c	0.03Ω	R_c	0.03Ω	3	0.23	0.318
L_c	0.35mH	L_c	0.35mH			
R_f	0.1Ω	R_f	0.1Ω			
L_f	1.35mH	L_f	1.35mH	**Loads**	**(kW)**	**L(mH)**
C_f	50μF	C_f	50μF	1	14	0.5
K_{pv}	0.1	K_{pv}	0.05	2	13	0.5
K_{iv}	420	K_{iv}	390	3	11	0.5
K_{pc}	15	K_{pc}	10.5	4	10	0.5
K_{ic}	20,000	K_{ic}	16,000			

VIII. RESULTS AND DISCUSSION

Results of the simulation work carried out are discussed under this section.

A. Performance Evaluation Under Load Perturbation Without Communication Impairments

This subsection evaluates the performance of the proposed voltage control scheme across three simulation stages:

- **Stage 1 (0.0 s ≤ t < 0.1 s):** Only the primary droop control is active, governing the voltage regulation of the DG units in a decentralized manner.
- **Stage 2 (0.1 s ≤ t < 0.3 s):** At $t = 0.1$ s, a step change in load is introduced by doubling the load on each DG unit through the addition of a 1 kW resistive load and a 0.5 mH inductive component across DG1 to DG4.
- **Stage 3 (t ≥ 0.3 s):** At $t = 0.3$ s, the consensus-based secondary voltage control scheme is activated and remains engaged for the remainder of the simulation.

The system's voltage control response is depicted in Figure 5. The results indicate that the primary droop control alone is weak for achieving voltage synchronization among the DG units, as voltage deviations persist across the network. Following the activation of the consensus-based secondary controller, the DG units reach a common voltage reference i.e., consensus within 1 second, demonstrating the effectiveness of the proposed scheme in coordinating voltage levels under dynamic load and communication conditions.

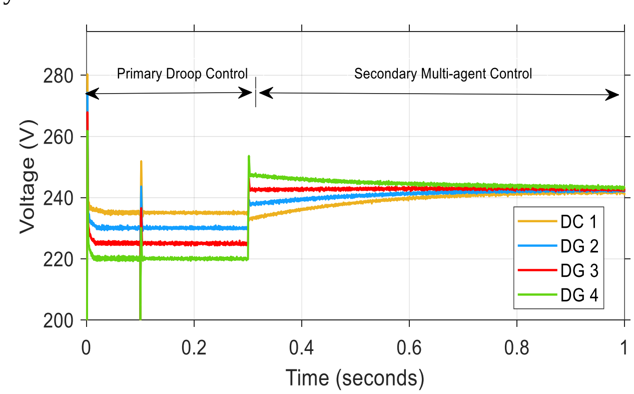

Figure 5: Voltage restoration and synchronization in d-component

In Figure 6, the three-phase output voltage waveforms equivalent of the d-component for each of the DGs are presented. The waveforms indicate that voltage restoration and synchronization was achieved with negligible distortion.

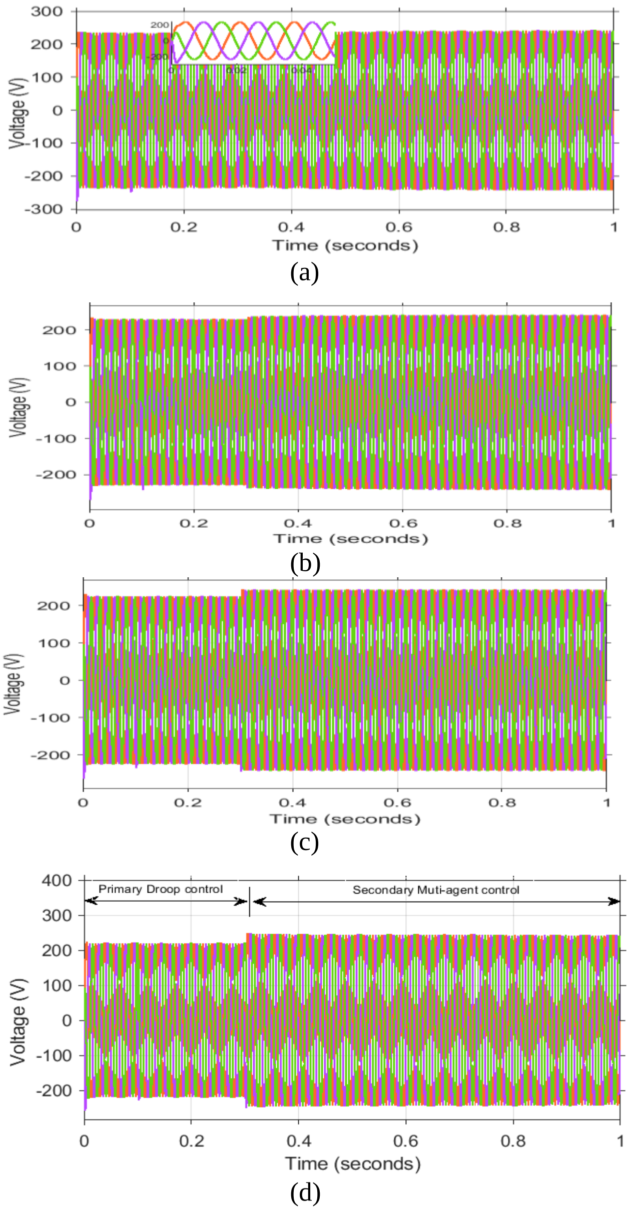

Figure 6: Tracking three-phase output voltage restoration of the DGs (a) DG 1; (b) DG 2; (c) DG 3; (d) DG 4

B. Performance with Communication Time Delays

To assess the robustness of the proposed control scheme under communication impairments, the system was subjected to varying levels of latency in the communication links among the DG units. Specifically, the voltage restoration performance was evaluated under the following delay conditions: τ_{t1} = 0.6 s, τ_{t2} = 0.7 s, τ_{t3} = 0.8 s, and τ_{t4} = 1.0 s. The simulation results, presented in Figure 7, demonstrate that the proposed consensus-based secondary control strategy successfully restores the DG terminal voltages to their nominal values despite the presence of communication delays. However, the time required to achieve voltage synchronization increases proportionally with the level of delay. Notably, at a maximum latency of 1.0 s, the system achieves voltage consensus approximately 3.3 seconds after activation of the secondary controller, representing a delay-induced degradation in convergence speed compared to the zero-latency scenario.

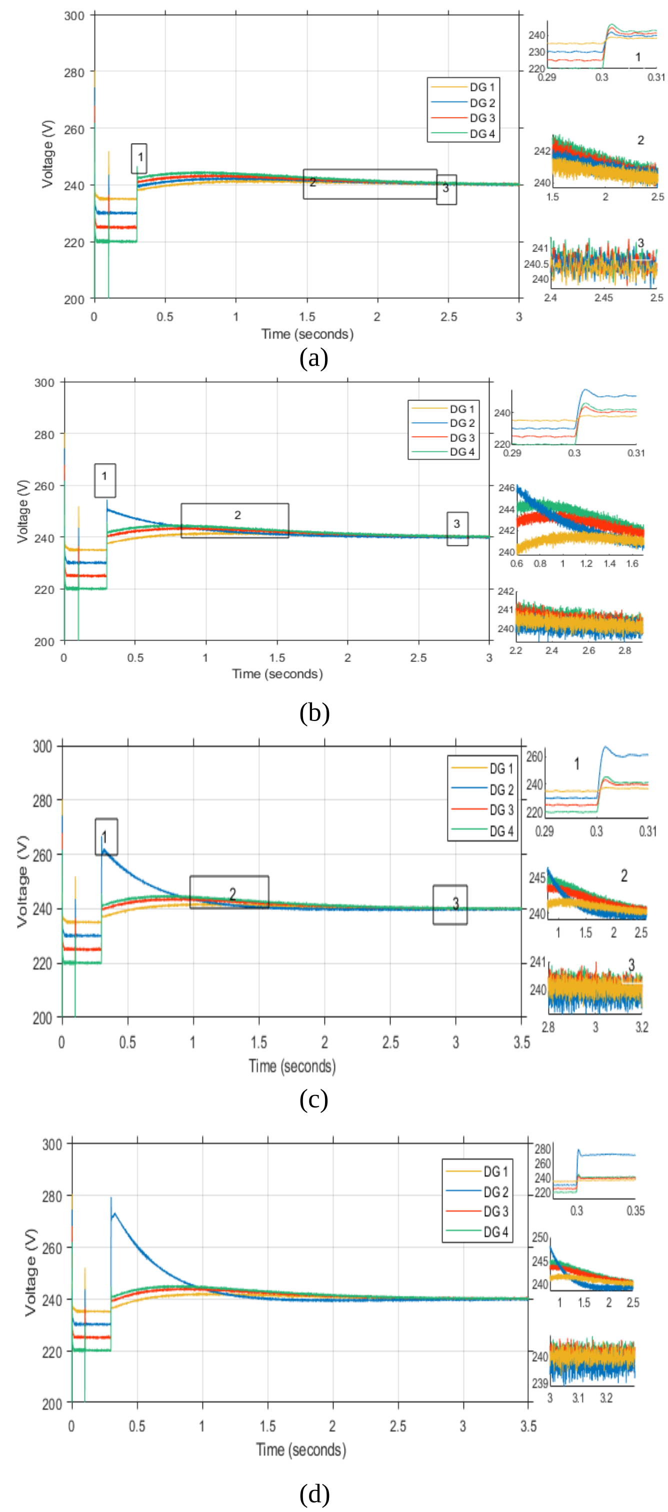

Figure 7: Tracking voltage restoration and synchronization performance of consensus control scheme under communication time delay (a) $\tau_{t1} = 0.6s$; (b) $\tau_{t2} = 0.7s$; (c) $\tau_{t3} = 0.8s$; and (d) $\tau_{t4} = 1.0s$

C. Performance Under Different Noise Level

The performance of the consensus-based secondary voltage control scheme under communication noise impairment was evaluated by introducing additive white Gaussian noise with varying noise variances, specifically σ^2 = 0.1, 0.2, 0.3, and 0.4. The voltage trajectories of the DG units under these noise conditions are illustrated in Figure 7. The results indicate that voltage synchronization was achieved across all scenarios, with an average convergence time of approximately 3 seconds. For lower noise levels (σ^2 = 0.1 and 0.2, shown in Figure 8(a) and Figure 8(b)), the DG voltages converged to the reference value shortly after activation of the secondary controller and remained stable thereafter, exhibiting negligible deviation. At higher noise levels (σ^2 = 0.3 and 0.4, Figure 8(c) and Figure 8(d)), slight deviations from the nominal voltage were observed due to increased measurement noise. Nevertheless, these deviations remained within acceptable tolerance margins, demonstrating the robustness of the proposed control strategy. Overall, the consensus-based scheme effectively maintained voltage synchronization despite the presence of communication noise.

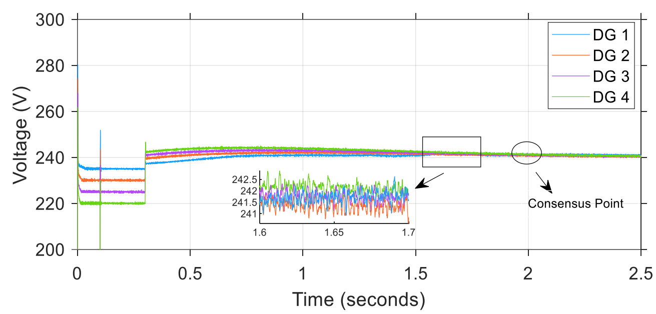

(a)

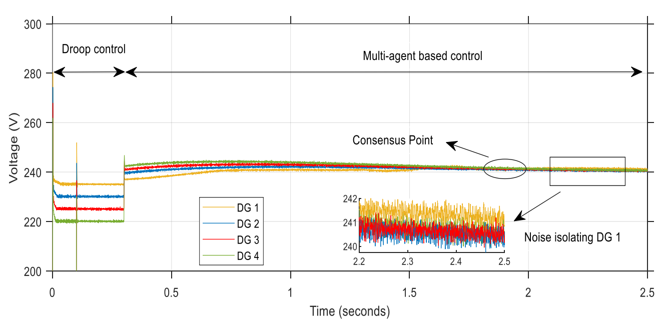

(b)

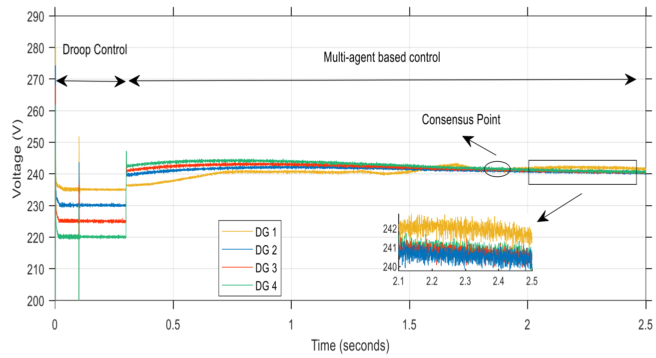

(c)

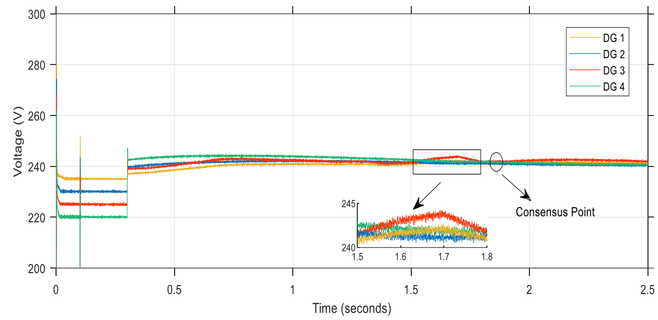

(d)

Figure 8: Consensus controller voltage performance tracking under noise impairment (a) $\sigma^2 = 0.1$; (b) $\sigma^2 = 0.2$; (c) $\sigma^2 = 0.3$; (d) $\sigma^2 = 0.4$

The performance of the developed consensus-based control scheme was evaluated on the three-phase output voltage waveforms shown in Figure 9 for all the connected DGs. The waveforms indicate that the noise impairment was mitigated by the proposed consensus control scheme; the distortions noticed were not significant while the DGs synchronization was taking place.

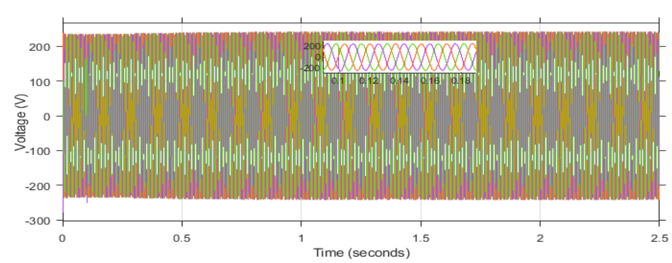

(a)

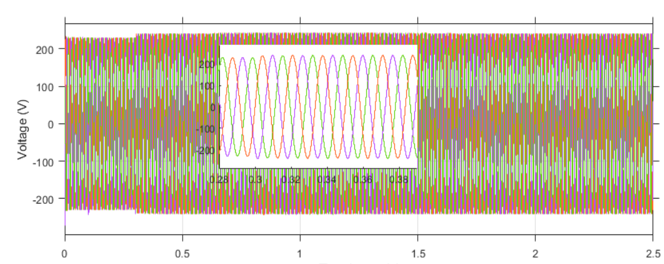

(b)

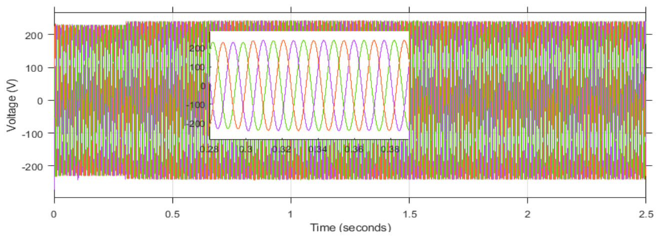

(c)

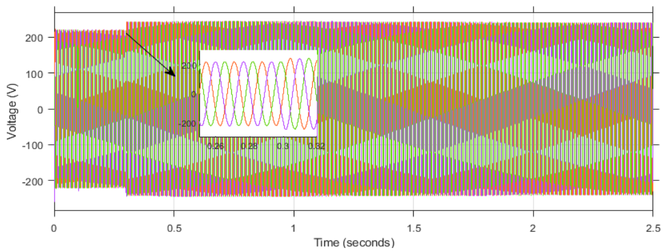

(d)

Figure 9: Tracking the performance of the consensus control scheme on the three-phase output voltage (a) DER 1; (b) DER 2; (c) DER 3; (d) DER 4

D. Performance with Combination of Link Noise and Delay

In this subsection, the performance of the consensus-based controller was evaluated under simultaneous conditions of communication link noise and latency. Figure 10 illustrates the controller's effectiveness in achieving voltage restoration and synchronization. The results demonstrate that the proposed controller successfully drives the microgrid (MG) toward consensus, maintaining performance within the acceptable distortion thresholds for inverter-based MGs. Nonetheless, the precise instant of consensus convergence becomes less discernible as the combined impact of communication delay and noise increases.

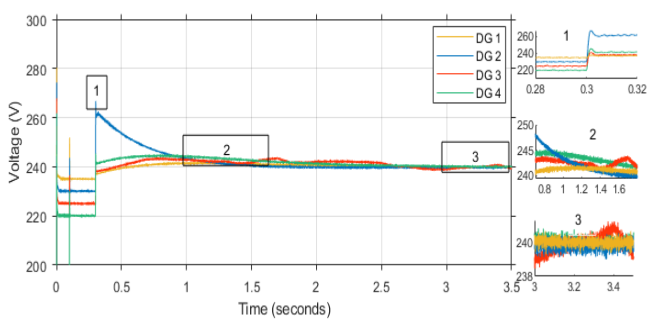

(a)

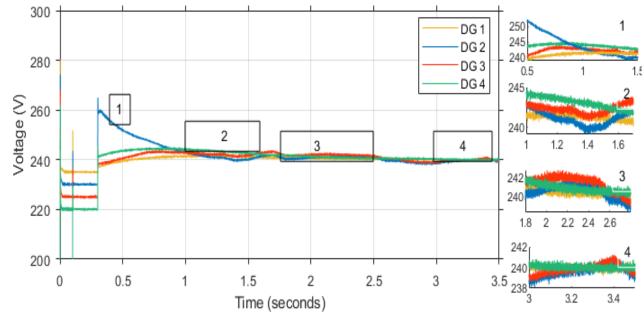

(b)

Figure 10: Tracking voltage restoration and synchronization performance of consensus control with link noise and link delay (a) τ_{t1} is 0.4sec. and σ^2 is 0.2; (b) τ_{t1} is 0.6sec. and σ^2 is 0.4

IX. CONCLUSION

A consensus-based secondary voltage control strategy has been proposed, simulated, and analyzed to achieve voltage synchronization and mitigate distortion in autonomous microgrids operating under communication link noise and delay. The simulation results underscore the effectiveness of the secondary control layer in managing voltage regulation and synchronization across distributed generation (DG) units. While the primary droop control maintains voltage distortion within permissible limits, it exhibits limitations in achieving voltage synchronization and equitable power sharing. The proposed consensus-based secondary control scheme effectively compensates for these deficiencies, achieving voltage consensus within 3 seconds, even under adverse conditions such as communication noise and delay. However, excessive noise levels in the communication network may compromise system stability, highlighting the necessity for robust communication protocols. Overall, the results validate the proposed method's capability to enhance microgrid resilience, ensuring reliable operation and improved power sharing performance among DG units in the presence of communication impairments.

AUTHOR CONTRIBUTIONS

S. A. Olayanju: Conceptualization, methodology, literature review, writing and analysis, review and editing. **F. M. Dahunsi and A. A. Ponnle**: Supervision, analysis and revising, review and editing. All authors have read and approved the manuscript.

REFERENCES

Aghaee, F., Dehkordi, N. M., Bayati, N., and Hajizadeh, A. (2019). Distributed control methods and impact of communication failure in AC microgrids: A comparative review. In *Electronics (Switzerland)* (Vol. 8, Issue 11, pp. 1–22).

Ahmed, K., Seyedmahmoudian, M., Mekhilef, S., Mubarak, N. M., and Stojcevski, A. (2021). A Review on Primary and Secondary Controls of Inverter-interfaced

Microgrid. In *Journal of Modern Power Systems and Clean Energy* (Vol. 9, Issue 5, pp. 969–985).

Ali, B., Nasirian, V., Davoudi, A., and Lewis, F. L. (2017). Cooperative Synchronization in Distributed Microgrid Control. In *Intelligent Microgrid Management and EV Control Under Uncertainties in Smart Grid* (Vol. 1, Issue April).

Aluko, A., Buraimoh, E., Oni, O. E., and Davidson, I. E. (2022). Advanced Distributed Cooperative Secondary Control of Islanded DC Microgrids. *Energies*, *15*(11), 1–17.

Andreotti, A., Caiazzo, B., Petrillo, A., and Santini, S. (2021). Distributed Robust Finite-Time Secondary Control for Stand-Alone Microgrids with Time-Varying Communication Delays. *IEEE Access*, *9*, 59548–59563.

Chen, M., Xiao, X. (2018). Secondary voltage control in islanded microgrids using event-triggered control. *IET Generation, Transmission and Distribution*, *12*(8), 1872–1878.

Dehkordi, N. M., Baghaee, H. R., Sadati, N., and Guerrero, J. M. (2019). Distributed Noise-Resilient Secondary Voltage and Frequency Control for Islanded Microgrids. *IEEE Transactions on Smart Grid*, *10*(4), 3780–3790.

Hu, J., and Bhowmick, P. (2020). A consensus-based robust secondary voltage and frequency control scheme for islanded microgrids. *International Journal of Electrical Power and Energy Systems*, *116*(September 2019), 1–11.

Huang, X., Fan, Y., Wu, H., Zhang, G., Yin, Z., Khan, M. Y. A., Liu, H., and Zhai, J. (2024). Distributed Secondary Control for Islanded Microgrids Considering Communication Delays. *IEEE Access*, *12*(April), 64335–64350.

Jasim, A. M., Jasim, B. H., Aymen, F., Kotb, H., and Althobaiti, A. (2023). Consensus-Based Intelligent Distributed Secondary Control for Multiagent Islanded Microgrid. *International Transactions on Electrical Energy Systems*, *2023*(1), 1–20.

Lakshminarayanan, V., Sekar, V. C., and Rajashekara, K. (2016). Novel communication architecture for Multi-Agent Systems in autonomous Microgrid. *IEEE Power and Energy Society General Meeting*, *2016-Novem*.

Li, W., Zhang, M., and Deng, Y. (2022). Consensus-Based Distributed Secondary Frequency Control Method for AC Microgrid Using ADRC Technique. *Energies*, *15*(9).

Lou, G., Gu, W., Lu, X., Xu, Y., and Hong, H. (2020). Distributed Secondary Voltage Control in Islanded Microgrids with Consideration of Communication Network and Time Delays. *IEEE Transactions on Smart Grid*, *11*(5), 3702–3715.

Lou, G., Gu, W., Sheng, W., Song, X., and Gao, F. (2018). Distributed model predictive secondary voltage control of islanded microgrids with feedback linearization. *IEEE Access*, *6*, 50169–50178.

Mallery, J., Bossuyt, D. L. Van, and Pollman, A. (2022). Defense Installation Energy Resilience for Changing Operational Requirements. *Designs*, 1–27.

Nasirian, V., Moayedi, S., Davoudi, A., and Lewis, F. L. (2015). Distributed cooperative control of dc microgrids. *IEEE Transactions on Power Electronics*, *30*(4), 2288–2303.

Olayanju, S. A., Dahunsi, F. M., and Ponnle, A. A. (2021). Mitigation strategies for communication networks induced impairments in autonomous microgrids control : A review. *AIMS Electronics and Electrical Engineering*, *5*(4), 342–375. https://doi.org/10.3934/electreng.2021018

Olayanju, S. A., Dahunsi, F. M., and Ponnle, A. A. (2024). Evaluation of Cross-Coupling Decoupling in Islanded Microgrid Control with Inductor Current Feed-Forward Technique. *EECCIS*, *18*(3), 107–116.

Olfati-Saber, R., and Murray, R. M. (2004). Consensus problems in networks of agents with switching topology and time-delays. *IEEE Transactions on Automatic Control*, *49*(9), 1520–1533.

Pogaku, N., Prodanović, M., and Green, T. C. (2007). Modeling, analysis and testing of autonomous operation of an inverter-based microgrid. *IEEE Transactions on Power Electronics*, *22*(2), 613–625.

Pompodakis, E. E., Orfanoudakis, G. I., Yiannis, K., and Karapidakis, E. S. (2024). Robust Secondary Controller for Islanded Microgrids with Unexpected Electrical Partitions under Fault Conditions. *Energies*, *17*(15).

Seyedmohammad Hasheminasab;, ; M. A., and Chaoui, H. (2024). A Review of Control Techniques for Inverter-Based Distributed Energy Resources Applications. *Energies*, 1–39.

Sheykhi, N., Salami, A., Guerrero, J. M., Agundis-Tinajero, G. D., and Faghihi, T. (2022). A comprehensive review on telecommunication challenges of microgrids secondary control. *International Journal of Electrical Power and Energy Systems*, *140*.

Shrivastava, S., Subudhi, B., and Das, S. (2019). Noise-resilient voltage and frequency synchronisation of an autonomous microgrid. *IET Generation, Transmission and Distribution*, *13*(2), 189–200.

Wu, X., Xu, Y., He, J., Shen, C., Chen, G., Vasquez, J. C., and Guerrero, J. M. (2019). Delay-Dependent Small-Signal Stability Analysis and Compensation Method for Distributed Secondary Control of Microgrids. *IEEE Access*, *7*, 170919–170935.

Yasir, M., Khan, A. L. I., Liu, H., Member, S., Zhang, Y., and Wang, J. (2024). Hybrid AC / DC Microgrid : Systematic Evaluation of Interlinking Converters , Control Strategies , and Protection Schemes : A Review. *IEEE Access*, *12*(November), 160097–160132.

Zhang, H., Kim, S., Sun, Q., and Zhou, J. (2017). Distributed Adaptive Virtual Impedance Control for Accurate Reactive Power Sharing Based on Consensus Control in Microgrids. *IEEE Transactions on Smart Grid*, *8*(4), 1749–1761.